On the structure of existence regions for sinks of the Hénon map

Zbigniew Galias[1,a)] and Warwick Tucker[2,b)]
[1]*Department of Electrical Engineering, AGH University of Science and Technology, al. Mickiewicza 30, Kraków 30–059, Poland*
[2]*Department of Mathematics, Uppsala University, Box 480, Uppsala 751 06, Sweden*

(Received 11 October 2013; accepted 21 January 2014; published online 18 February 2014)

An extensive search for stable periodic orbits (sinks) for the Hénon map in a small neighborhood of the classical parameter values is carried out. Several parameter values which generate a sink are found and verified by rigorous numerical computations. Each found parameter value is extended to a larger region of existence using a simplex continuation method. The structure of these regions of existence is investigated. This study shows that for the Hénon map, there exist sinks close to the classical case. © *2014 AIP Publishing LLC*. [http://dx.doi.org/10.1063/1.4865110]

The goal of the theory of dynamical systems is to give a description of the long-term behaviour of a given system. Invariant sets such as fixed points, periodic points, Smale horseshoes, and more complicated, strange attractors are examples of sets that remain present after the transient behaviour of the system has settled down. Of these invariant sets, only the ones that are attracting are detectable in some physical sense. In this paper, we study the presence of stable periodic orbits (sinks) for the Hénon map. The main challenge is to locate such sinks as they have very small regions of existence. Here we demonstrate that there exist low-period sinks extremely close to the classical parameter values of the Hénon map. Our conclusion is that most numerical studies to this date do not display anything but transient behaviour and are therefore inconclusive as to the true nature of the long-term dynamics of the Hénon map.

I. INTRODUCTION

The Hénon map[1] is a two-parameter, invertible map of the plane defined by

$$h(x,y) = (1 + y - ax^2, bx). \tag{1}$$

Originally designed to model the Poincaré map of the Lorenz flow, it displays a wide array of dynamical behaviors as its parameters are varied. For the classical parameter values, $(\bar{a},\bar{b}) = (1.4, 0.3)$ the so-called Hénon attractor is observed (see Fig. 1).

Despite almost 40 years of extensive study, the long term dynamics of the Hénon map remains unknown; it has not been established whether or not the map has a strange attractor for the classical parameter values.

For $b = 0$, the Hénon map reduces to the quadratic map $f_a(x) = 1 - ax^2$. Today, the dynamics of this map is well understood: its parameter space can be partitioned into two large sets $\mathcal{S}^+$ and $\mathcal{S}^-$. For $a \in \mathcal{S}^+$ the map f_a is chaotic, meaning that the dynamics supports a unique absolutely continuous invariant measure. For $a \in \mathcal{S}^-$ the dynamics is regular, meaning that the attracting set is a unique periodic sink. By a series of very deep results,[2–4] it is known that $\mathcal{S}^-$ is open and dense, $\mathcal{S}^+$ is a Cantor set having positive Lebesgue measure, and that $\mathcal{S}^+ \cup \mathcal{S}^-$ has full one-dimensional measure in the parameter space for a.

For $b \neq 0$, the sets of regular and chaotic parameters can be extended into the two-dimensional parameter space. In what follows, we will only consider positive values of b.

For $b > 0$ sufficiently small, it is known[5] that the Hénon map has a strange attractor for all $a \in \mathcal{A}_b$, where $\mathcal{A}_b$ has positive Lebesgue measure. As a consequence, the set $\mathcal{S}^+$ has positive two-dimensional Lebesgue measure for the Hénon map.

For $0 < b < 1$ it is known[6] that when a saddle point generates a homoclinic intersection, a cascade of (periodic) sinks will occur. Furthermore, there are parameters a such that the Hénon map (unlike the quadratic map) has infinitely many co–existing sinks.[7] Nevertheless, coexisting sinks for the Hénon map appear to be very elusive; because of the dissipative nature of the map, the regions in the parameter space for which sinks appear simultaneously are extremely small. In Ref. 8, a search for parameter values for which there exist at least three attractors was performed. Based on these results, it is believed that the sets $\mathcal{S}^+$ and $\mathcal{S}^-$ may overlap, i.e., there may exist parameters for which periodic sinks co–exist with a strange attractor.

Since the set of chaotic parameters $\mathcal{S}^+$ has positive measure, a parameter picked at random has a positive probability of belonging to $\mathcal{S}^+$. However, if the situation of the quadratic map carries over to that of the Hénon map, then $\mathcal{S}^+$ has empty interior, which means that an arbitrarily small perturbation can bring a parameter in $\mathcal{S}^+$ to the set of regular parameters $\mathcal{S}^-$. With our knowledge today, it therefore seems very unlikely that a specific point in parameter space can be verified to belong to $\mathcal{S}^+$. On the other hand, $\mathcal{S}^-$ is an open set. As such, membership to this set should be verifiable with a limited amount of information.

In view of this, we are prepared to state the following, perhaps unexpected, conjecture:

Conjecture: For the classical parameter values, the Hénon attractor is a periodic sink.

a)Electronic mail: galias@agh.edu.pl.
b)Electronic mail: warwick@math.uu.se.

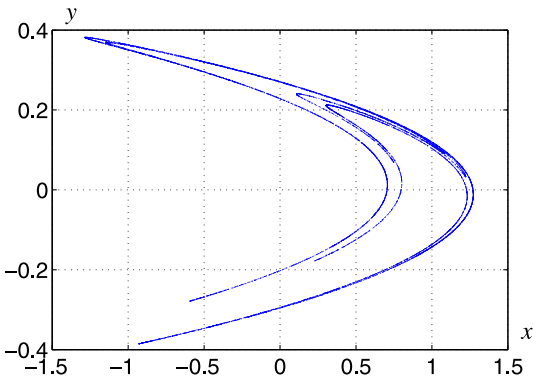

FIG. 1. $a = 1.4$, $b = 0.3$, trajectory of the Hénon map composed of 10 000 points.

This appears to be contradicted by numerical simulations such as the one illustrated in Figure 1. However, chaotic (or near-chaotic) maps are very hard to simulate accurately, and there is no real reason to trust the results of such computations. In fact, from a statistical point of view, there is a positive probability that the Hénon attractor is periodic, i.e., what we observe in computer simulations is actually a transient behaviour to a periodic steady state or a periodic orbit with a very long period. If this is true, then—in principle—we should be able to prove this fact. Verifying the existence of a sink involves only a finite amount of computations, and all necessary conditions are robust (there exists an open set in the parameter space in which all conditions remain true).

In this work, we present the results of a numerical search for parameter values—close to the classical ones—for which there exists a sink. Preliminary results of this study were reported in Ref. 9. We succeed in locating a number of such parameter values in a neighborhood of $(\bar{a}, \bar{b}) = (1.4, 0.3)$. Our study shows that, close to the classical case, the regions of existence of sinks are very narrow, and finding them is not a trivial numerical task. Moreover, we show that in many cases where there appears to be a strange attractor, the true underlying dynamics is in fact governed by a low-period sink. Using a simplex continuation method, the region of existence of each found sink is extended, allowing us to move closer to the classical case.

As a motivation for our conjecture we state one of our findings:

Theorem: *The Hénon map supports a period-28 sink for the parameter values (a,b) = (1.4,0.2999999774905).*

II. NUMERICAL METHODS TO STUDY THE EXISTENCE OF SINKS

We say that the orbit $z = (z_0, z_1, \ldots, z_{p-1})$, $z_k = h(z_{k-1})$ for $k = 1, 2 \ldots, p-1$ is *periodic with period p* if $z_0 = h(z_{p-1})$ and $z_0 \neq h^k(z_0)$ for $0 < k < p$. We say that z is a *period-p sink* if z is periodic with period p and the trajectory z is asymptotically stable, i.e., for each $\varepsilon > 0$ there exists $\delta > 0$ such that if $\| \hat{z} - z_l \| < \delta$ for some $l = 0, 1, \ldots, p-1$ then $\| h^k(\hat{z}) - h^k(z_l) \| < \epsilon$ for all $k > 0$ and $\lim_{k\to\infty} \| h^k(\hat{z}) - h^k(z_l) \| = 0$.

A. Locating sinks

Sinks are periodic orbits which locally attract trajectories. The natural method to find a sink is to follow a trajectory and monitor whether it converges to a periodic orbit. First, a number of iterates are computed in the hope that a trajectory reaches a steady-state. The number of iterations which have to be discarded is usually chosen by trial-and-error. It depends on Lyapunov exponents along the orbit, the size and shape of its basin of attraction, etc. Next, we take the current iterate as the new initial point and check if the trajectory periodically returns very close to this point. If we detect such a trajectory, we have a candidate for a sink.

It is possible that an observed periodic behaviour is an artifact caused by rounding errors. Because the set of representable real numbers is finite, there is a non-zero probability that a trajectory found by a computer hits the same point twice (and then it will repeat itself for ever), even if there is no stable periodic orbit in its neighborhood. Examples will be given in Sec. III. To be sure that the sink exists, we first have to prove that there exist a periodic orbit in a neighborhood of the candidate and then that the orbit is asymptotically stable. The proofs will be carried out using methods from interval analysis.[10,11] Computations in properly rounded interval arithmetic produce results which contain both machine arithmetic results and also true (infinite arithmetic precision) results and therefore may be used to obtain rigorous results. Interval methods provide simple tests for the existence and uniqueness of zeros of a map within a given interval vector. To investigate zeros of $F : \mathbb{R}^n \mapsto \mathbb{R}^n$ in the interval vector $\boldsymbol{x}$ one evaluates an interval operator, for example, the interval Newton operator,[11] over $\boldsymbol{x}$

$$\mathrm{N}(\boldsymbol{x}) = \hat{x} - F'(\boldsymbol{x})^{-1} F(\hat{x}), \tag{2}$$

where $\hat{x} \in \boldsymbol{x}$, and $F'(\boldsymbol{x})$ is an interval matrix containing the Jacobian matrices $F'(x)$ for all $x \in \boldsymbol{x}$. The main theorem on the interval Newton operator states that if $\mathrm{N}(\boldsymbol{x}) \subset \boldsymbol{x}$, then F has exactly one zero in $\boldsymbol{x}$.

To study the existence of period- p orbits of h, we construct the map F defined by

$$F\begin{pmatrix} x_0 \\ x_1 \\ \vdots \\ x_{p-1} \end{pmatrix} = \begin{pmatrix} 1 - ax_0^2 + bx_{p-1} - x_1 \\ 1 - ax_1^2 + bx_0 - x_2 \\ \vdots \\ 1 - ax_{p-1}^2 + bx_{p-2} - x_0 \end{pmatrix}. \tag{3}$$

It is clear that $x = (x_0, x_1, \ldots, x_{p-1})$ is a zero of F if and only if $z_0 = (x_0, y_0) = (x_0, bx_{p-1})$ is a fixed point of h^p. To prove the existence of a periodic orbit in a neighborhood of the computer generated trajectory $x = (x_0, x_1, \ldots, x_{p-1})$, we choose the radius r, construct the interval vector $\boldsymbol{x} = (\mathbf{x}_0, \mathbf{x}_1, \ldots, \mathbf{x}_{p-1})$, where $\mathbf{x}_k = [x_k - r, x_k + r]$ and verify whether $\mathrm{N}(\boldsymbol{x}) \subset \boldsymbol{x}$. If the existence condition does not hold we may choose a different r and try again (see Ref. 12 for details). This method combined with the bisection technique has been used to find all short periodic orbits for discrete systems including the Hénon map[13] and continuous systems.[12]

The stability of the orbit $z = (z_0, z_1, \ldots, z_{p-1})$ depends on the eigenvalues $\lambda_{1,2}$ of the Jacobian matrix

$$J_p(z_0) = (h^p)'(z_0) = h'(h^{p-1}(z_0)) \cdots h'(h(z_0)) \cdot h'(z_0), \quad (4)$$

where $z_0 = (x_0, y_0) = (x_0, bx_{p-1})$. We will assume that the eigenvalues are ordered in such a way that $|\lambda_1| \geq |\lambda_2|$. If both eigenvalues lie within the unit circle, i.e., $|\lambda_1| < 1$ then the orbit is asymptotically stable. If at least one eigenvalue lies outside the unit circle ($|\lambda_1| > 1$) then the orbit is unstable.

Note that the Jacobian matrix of the Hénon map is

$$h'(x, y) = \begin{pmatrix} -2ax & 1 \\ b & 0 \end{pmatrix}, \quad (5)$$

and hence its determinant is $\det(h'(x, y)) = -b$. It follows that $\det(J_p(z_0)) = (-b)^p$, and $\lambda_1 \lambda_2 = (-b)^p$, so for $|b| < 1$ at least one of the eigenvalues lies within the unit circle.

B. Immediate basin of the attractor

Even if there exists a sink for given parameter values and there are no other attractors for the system, it may happen that we will not be able to locate the sink using arithmetic of a given precision (compare Ref. 14). This is a consequence of the fact that trajectories are guaranteed to be attracted to the sink only in its neighborhood. If the size of this neighborhood is smaller than the arithmetic precision we will perhaps never observe the sink in simulations. In this context a very important notion is the immediate basin of attraction.

We say that a point z belongs to the *immediate basin of attraction* $\mathrm{B}_\varepsilon(A)$ of the attractor A if its trajectory converges to the attractor and does not escape further than ε from it

$$\mathrm{B}_\varepsilon(A) = \{z : \mathrm{d}(h^n(z), A) \leq \varepsilon \forall n \geq 0 \text{ and } \lim_{n\to\infty} \mathrm{d}(h^n(z), A) = 0\}, \quad (6)$$

where $d(z,A)$ denotes the distance between the point z and the set A. The choice of ε is somewhat arbitrary. For attractors which are not fixed points, choosing ε to be a fraction (for example 1%) of the size of the attractor usually works well.

The probability that a trajectory converges to an attractor after a certain number of iterations depends on the area of its immediate basin of attraction. If the immediate basin of attraction has very small area, it will on average take many iterations for a trajectory to converge to the attractor. What we observe in such a case is a very long transient, which sometimes is misidentified as a chaotic trajectory.

It may be difficult/time-consuming to find an accurate approximation of the immediate basin of attraction and its area. However, for periodic attractors, we can easily find a set enclosed in the immediate basin. Let us define the *radius of the immediate basin at point z* as

$$\mathrm{r}_\varepsilon(z) = \sup\{r : \mathrm{D}(z, r) \subset \mathrm{B}_\varepsilon(A)\}, \quad (7)$$

where $\mathrm{D}(z,r)$ denotes the disk with the radius r centered at z. As a lower bound of the immediate basin area of the periodic attractor $A = (z_0, z_1, \ldots, z_{p-1})$, we will use the area of disks centered at z_k with radii $r_k = \mathrm{r}_\varepsilon(z_k)$

$$\mathrm{s}_\varepsilon(A) = \mathrm{area}\left(\bigcup_{k=0,1,\ldots p-1} \mathrm{D}(z_k, r_k)\right). \quad (8)$$

Since usually the radii r_k are very small and in consequence the disks $\mathrm{D}(z_k,r_k)$ do not overlap, $\mathrm{s}_\varepsilon(A)$ can be computed as

$$\mathrm{s}_\varepsilon(A) = \sum_{k=0,1,\ldots p-1} \pi \mathrm{r}_\varepsilon(z_k)^2. \quad (9)$$

Another important parameter describing the basin of attraction is the *minimum immediate basin radius* $\mathrm{r}_\varepsilon(A)$ of the attractor, which is defined as the largest number such that all points lying closer than r_ε from the attractor belong to the immediate basin of attraction

$$\begin{aligned} \mathrm{r}_\varepsilon(A) &= \sup\{r : x \in \mathrm{B}_\varepsilon(A) \text{ for all } \mathrm{d}(x, A) \leq r\} \\ &= \inf\{\mathrm{r}_\varepsilon(z) : z \in A\}. \end{aligned} \quad (10)$$

The minimum immediate basin radius tells us how much we can perturb a point on the attractor so that its trajectory does not leave a neighborhood of the attractor. If the minimum immediate basin radius is smaller than the arithmetic precision used, then it is likely that we will not be able to detect the attractor by monitoring system's trajectories.

For a periodic attractor $A = (z_0, z_1, \ldots, z_{p-1})$ the minimum immediate basin radius can be computed as

$$\mathrm{r}_\varepsilon(A) = \min_{k=0,1,\ldots p-1} \mathrm{r}_\varepsilon(z_k), \quad (11)$$

where $\mathrm{r}_\varepsilon(z_k)$ are defined in (7).

C. Continuation method to find sink existence regions

When a point (a,b) in the parameter space with a sink is found one may use the continuation method to find a connected region in the parameter space for which this sink exists. The simplest version of the continuation method is to select grid points $(a + k \cdot \Delta a, b + l \cdot \Delta b)$, $k, l \in \mathbb{Z}$ in the parameter space and continue to neighboring grid points from the set of active grid points. The search procedure is initiated with the set of active grid points containing the initial point (a,b). Note that it is not necessary to run long computations to find the steady state for a neighboring grid point. Since the position of the orbit changes continuously with the parameters, the position of the sink for a new point can be found using the standard (real valued) Newton method started at the position of the orbit for the current point in the parameter space. This method has an advantage that it is robust and can be applied to find the existence regions of arbitrary shape. It has been used in Ref. 8 to find complex existence regions of various sinks for the Hénon map in the parameter range $(a, b) \in [0, 1.5] \times [0, 0.5]$.

Another approach is to find the border of the existence region. If it works, it is usually much faster since the number of test points, which has to be considered to locate the region with a given precision is significantly reduced (instead of

finding grid points filling the two-dimensional region, we have to find an approximate position of the border (a one-dimensional object). The border is defined by two conditions. The first condition is that the periodic orbit exists, and the second condition is that the largest (in absolute value) eigenvalue of the Jacobian matrix has the absolute value equal to 1. To implement this idea, we first locate two points belonging to the border of the existence region. This is done by continuing from the point in which the sink exists in two arbitrarily chosen opposite directions. Then, for each border point, we use the simplex continuation method[15] to locate the border. In this continuation method, a sequence of triangles is constructed such that each triangle has non-empty intersection with the border. Corners of the triangles are located on a regular grid. As the first triangle we choose the one containing the border point found in the initial step. Assuming that two edges of this triangle have nonempty intersection with the existence region we continue in two directions. In each direction the initial triangle is replaced by the triangle defined by two corners of the chosen edge, and the third corner is a grid point located symmetrically to the third point of the initial triangle. This process is repeated and a sequence of triangles containing the border is found. This method allowed us to find existence regions of several sinks for parameter values close to the classical case.[9] However, this method can be very slow especially when the existence regions are narrow. The reason is that for a narrow region, the grid points have to be very close to each other. As it will be shown in Sec. III, some of the regions have width below 10^{-13}. To have a good chance that the simplex continuation method works properly, grid points should lie in an order of magnitude closer to each other than the width of the existence region. This results in very low speed of moving in the parameter space.

Below, we present a version of the continuation method designed to work for very thin regions. It works for existence regions locally resembling a stripe.

The first improvement to implement the continuation method in a more efficient way is based on obtaining a better approximation of the position of the sink for a new test point. Let us assume that for the current point (a,b) in the parameter space the position of the sink is $x=(x_0,x_1,\ldots,x_{p-1})$. In the simplest approach one may use $\tilde{x}=x$ as a guess of the position of the sink for the test point $(\tilde{a},\tilde{b})=(a+\Delta a,b+\Delta b)$. A better approximation can be obtained using the implicit function theorem applied to the equation $F(x)=0$, where $x=(x_0,x_1,\ldots,x_{p-1})$ and F is defined in (3). From the implicit function theorem, it follows that if the matrix

$$\frac{\partial F}{\partial x}=\begin{pmatrix} -2ax_0 & -1 & 0 & \cdots & 0 & b \\ b & -2ax_1 & -1 & \cdots & 0 & 0 \\ 0 & b & -2ax_2 & \cdots & 0 & 0 \\ \vdots & \vdots & \vdots & \ddots & \vdots & \vdots \\ 0 & 0 & 0 & \cdots & -2ax_{p-2} & -1 \\ -1 & 0 & 0 & \cdots & b & -2ax_{p-1} \end{pmatrix}$$

is invertible, then the partial derivatives $\partial x/\partial a=(\partial x_0/\partial a,\partial x_1/\partial a,\ldots,\partial x_{p-1}/\partial a)^T$ of the solution $x(a,b)$ of $F(x)=0$ can be obtained by solving the linear equation

$$\frac{\partial F}{\partial x}\cdot\frac{\partial x}{\partial a}+\frac{\partial F}{\partial a}=0, \tag{12}$$

where $\partial F/\partial a=(-x_0^2,-x_1^2,\ldots-x_{p-1}^2)^T$.

Similarly, the partial derivatives $\partial x/\partial b$ can be obtained by solving the equation

$$\frac{\partial F}{\partial x}\cdot\frac{\partial x}{\partial b}+\frac{\partial F}{\partial b}=0, \tag{13}$$

where $\partial F/\partial b=(x_{p-1},x_0,\ldots x_{p-2})^T$.

Once the derivatives $\partial x/\partial a$ and $\partial x/\partial b$ are known, a better approximation of the position of the orbit for the test point $(\tilde{a},\tilde{b})=(a+\Delta a,b+\Delta b)$ can be constructed as

$$\tilde{x}=x+\frac{\partial x}{\partial a}\cdot\Delta a+\frac{\partial x}{\partial b}\cdot\Delta b. \tag{14}$$

This better approximation is used as an initial point for the Newton method to find an accurate approximation of the position of the sink for the test point $(\tilde{a},\tilde{b})$. Since the convergence of the Newton method depends of the quality of the initial point, more distant points in the parameter space can be tested and, as a consequence, we can move faster in the parameter space.

The second improvement is based directly on the assumption that the existence region locally resembles a stripe. The idea is based on the observation that the direction of the stripe locally agrees with the direction in which the maximum eigenvalue of the orbit is constant (compare also the notion of spine locus introduced in Ref. 16).

For the current point (a,b) in the parameter space we compute the eigenvalues $\lambda_{1,2}$ of the Jacobian matrix (4) and their derivatives $\partial\lambda_{1,2}/\partial a$, $\partial\lambda_{1,2}/\partial b$ with respect to the parameters a, b. The derivatives can be easily obtained using automatic differentiation and derivatives $\partial x/\partial a$, and $\partial x/\partial b$ computed from (12) and (13). Let λ_1 be the eigenvalue with largest absolute value. Close to the point (a,b) this eigenvalue is approximately equal to

$$\lambda_1(a+\Delta a,b+\Delta b)\approx\lambda_1(a,b)+\frac{\partial\lambda_1}{\partial a}\cdot\Delta a+\frac{\partial\lambda_1}{\partial b}\cdot\Delta b.$$

If we continue in the directions $(\Delta a,\Delta b)=\pm(\partial\lambda_1/\partial a,\partial\lambda_1/\partial b)$, we will reach the borders of the existence region. If we continue in the directions $(\Delta a,\Delta b)=\pm(\partial\lambda_1/\partial b,-\partial\lambda_1/\partial a)$ we move along the existence region. This way we can move much further in one step than in the previous method.

Summarizing, the procedure we use is following. From the current point we find border points of the existence region continuing in the directions $(\Delta a,\Delta b)=\pm(\partial\lambda_1/\partial a,\partial\lambda_1/\partial b)$. Then we find the center of the existence region and from this point we continue as far as possible in the directions $(\Delta a,\Delta b)=\pm(\partial\lambda_1/\partial b,-\partial\lambda_1/\partial a)$. This gives us another point belonging to the existence region, and the procedure is repeated as long as we stay in the region of interest.

III. RESULTS

A. Exhaustive search for sinks

In order to locate sinks for parameter values close to the classical ones $(\bar{a},\bar{b}) = (1.4, 0.3)$, we have carried out a number of search tests. Since the goal of this study is to investigate the structure of regions of existence of sinks close to the classical case, the search was limited to the rectangle $(a,b) \in [1.3999, 1.4001] \times [0.2999, 0.3001]$. As it will be shown later in most cases existence regions are narrow stripes crossing the region of interest. Taking this into account, it seems to be a good idea to search for sinks at points located uniformly along straight lines. This way is more systematic than using randomly selected points and hopefully will enable us to locate more sink existence regions and formulate more reliable conclusions.

When a candidate for a sink is found, we attempt to prove the existence of a sink for this parameter value using the interval Newton method. For shorter orbits we use the standard double-precision interval arithmetic. For longer orbits with period $p > 40$ multiple precision arithmetic with the precision of 200 bits is used. Once the existence of a sink is confirmed, the corresponding periodic window within the search interval is found non-rigorously using the continuation method. The positions of windows are recorded, and when a new candidate is found to belong to one of the existing windows, it is skipped. In this way, for most sink candidates we are able to either prove the existence of a sink or to find a window containing the sink.

In some very rare cases (146 out of 820 958 candidates) the Newton method fails and there is no known window containing the sink candidate. The failure could be caused by two factors. The first one is the possibility that a computer generated trajectory hits exactly the same representable numbers (computation artifact) and therefore appears to be a periodic orbit. It is also possible that there exist an attractor very close to the computer generated trajectory, but its period is very high or infinite (chaotic attractor). Such attractors can be created via a sequence of period doubling bifurcations.

An example of the first case is the period-92 sink candidate $(x_0,y_0) = 1.01699439297806,0.10713546854902)$ found for $(a,b) = (1.4,0.299999988104045)$. Using rigorous computations, it is confirmed that there is a period-92 orbit close to this initial condition, but the orbit is unstable. Moreover, when the computations are carried out in higher precision, then no sink candidate is found. This indicates that the sink candidate is a result of rounding errors. This example shows that proving the existence of a sink is a necessary step of the search procedure.

An example of the second case is observed for $(a,b) = (1.399983677314,0.3001)$. In this case, a period-76 sink candidate at $(x_0,y_0) = (1.2715021944,–0.020761622165)$ is found. As in the previous case, we prove that there is an unstable period-76 orbit close to this initial condition. In contrast to the previous case, however, higher precision computations reveal the same sink candidate. For this case, we are able to prove the existence of a trapping region enclosing the unstable period-76 orbit. The existence of the trapping region is established using techniques introduced in Ref. 8. The trapping region is composed of 1241 487 rectangles (interval vectors) of size $5 \cdot 10^{-9} \times 5 \cdot 10^{-9}$. When plotted, the trapping region looks like 19 dots, but in fact it is composed of 19 connected regions, which in a close-up appear to be very short intervals or arcs. These regions are small; the diameter of the largest of them is less than 0.0009. The attractor residing in the trapping region may be chaotic.

Several search tests have been carried out. In each search test we have selected a large number n_{par} of points uniformly filling an interval in the parameter space. For each parameter point considered, we have randomly selected n_{init} initial conditions and for each initial condition n_{skip} iterations were computed and skipped to reach the steady state and the following $n_{\text{iter}} = 10\,000$ iterations were used to verify whether the trajectory in the steady state is periodic as described in Sec. II A. The total number of iterations in a search test is approximately $n_{\text{par}} \cdot n_{\text{init}} \cdot n_{\text{skip}}$ and ranges from 10^{11} to 10^{18}. The search was limited to sinks with period less than 200. Most computations were performed using the GPU architecture. We tested whether one should compute one very long trajectory or many shorter trajectories starting from random initial conditions. The tests showed that what matters is the total number of iterations (i.e., $n_{\text{init}} \cdot n_{\text{skip}}$). The search procedure with many randomly chosen initial conditions was used because it is easier to parallelize.

Computation details and results obtained for different search tests are presented in Table I. For each search test we report the search interval, the numbers n_{par}, n_{init}, and n_{skip}, the number n_{sink} of parameter values with a sink found and the number n_{win} of periodic windows. In the description of the interval in the parameter plane we use the shorthand notation, where for example $1.^{4001}_{3999} \times 0.3$ denotes the interval $[1.3999,1.4001] \times [0.3,0.3]$. We have performed search for sinks in three horizontal intervals: $[1.3999,1.4001] \times [0.3]$, $[1.3999,1.4001] \times [0.2999]$, $[1.3999,1.4001] \times [0.3001]$, and one vertical interval $\{1.4\} \times [0.2999,0.3001]$, all of length $2 \cdot 10^{-4}$ (tests #1–5, 27–28, 29–30, and 18–20). We have also considered shorter intervals passing through the point $(a,b) = (1.4,0.3)$ to detect more sinks in a smaller neighborhood of the point of classical parameter values (tests #6–17 and 21–26).

Let us now see how the parameters of the search procedure influence the results. In the first five search tests the same search interval $[1.3999,1.4001] \times [0.3]$ is used. When n_{par} grows the number n_{sink} of parameter values with a sink grows, and the growth rate is roughly proportional ($n_{\text{par}} = 2 \cdot 10^7$ gives $n_{\text{sink}} = 850$ in test #2 and $n_{\text{par}} = 2 \cdot 10^8$ gives $n_{\text{sink}} = 8502$ in the test #5). This is expected since n_{sink} grows linearly when more points are added inside periodic windows. However, note that the number of periodic windows grows only by a factor of 2 (from 63 to 134). Second, let us compare the influence of the parameter n_{skip} on the results. In the test #3 four times more initial conditions were used than in the test #2. The result n_{sink} grows from 850 to 862, which is little when one takes into account the fact that the computation time is four times longer. However, this increase is associated mostly with new periodic windows (the number n_{win} grows from 63 to 73). The conclusion is that increasing iteration number for a given point in the

TABLE I. Computation details of search for sinks $(a,b) \in$ close to $a=1.4$, $b=0.3$.

	$a \times b$	n_{par}	n_{init}	n_{skip}	n_{sink}	n_{win}
1	$1.^{4001}_{3999} \times 0.3$	$1 \cdot 10^6$	1000	$2 \cdot 10^6$	44	16
2		$2 \cdot 10^7$	1000	10^6	850	63
3		$2 \cdot 10^7$	1000	$4 \cdot 10^6$	862	73
4		$8 \cdot 10^7$	1000	10^6	3396	101
5		$2 \cdot 10^8$	1000	10^6	8502	134
6	$1.^{40001}_{39999} \times 0.3$	$1 \cdot 10^6$	1000	10^5	3	1
7		$2 \cdot 10^7$	1000	10^6	79	9
8		$2 \cdot 10^8$	1000	10^6	730	18
9	$1.^{400001}_{399999} \times 0.3$	$1 \cdot 10^6$	1000	10^5	0	0
10		$2 \cdot 10^6$	2000	10^5	1	1
11		$2 \cdot 10^7$	1000	10^6	4	1
12		$2 \cdot 10^8$	1000	10^5	8	2
13		$2 \cdot 10^8$	1000	10^6	53	8
14	$1.^{4000001}_{3999999} \times 0.3$	$1 \cdot 10^6$	2000	10^5	0	0
15		$2 \cdot 10^8$	1000	10^6	9	2
16	$1.^{400000025}_{399999975} \times 0.3$	$1 \cdot 10^8$	1000	10^7	0	0
17	$1.^{40000001}_{39999999} \times 0.3$	$2 \cdot 10^8$	1000	10^6	0	0
18	$1.4 \times 0.^{3001}_{2999}$	$2 \cdot 10^7$	1000	10^6	15989	82
19		$2 \cdot 10^7$	1000	$4 \cdot 10^6$	16001	92
20		$2 \cdot 10^8$	1000	10^6	159835	185
21	$1.4 \times 0.^{30001}_{29999}$	$2 \cdot 10^8$	1000	10^6	8649	39
22	$1.4 \times 0.^{300001}_{299999}$	$2 \cdot 10^7$	1000	10^6	1	1
23		$2 \cdot 10^8$	1000	10^6	2	1
24	$1.4 \times 0.^{3000001}_{2999999}$	$2 \cdot 10^8$	1000	10^6	8	2
25	$1.4 \times 0.^{300000025}_{299999975}$	$1 \cdot 10^8$	1000	10^7	123	3
26	$1.4 \times 0.^{30000001}_{29999999}$	$2 \cdot 10^8$	1000	10^6	0	0
27	$1.^{4001}_{3999} \times 0.3001$	$2 \cdot 10^7$	1000	10^6	54810	79
28		$2 \cdot 10^8$	1000	10^6	548148	153
29	$1.^{4001}_{3999} \times 0.2999$	$2 \cdot 10^7$	1000	10^6	246	41
30		$2 \cdot 10^8$	1000	10^6	2459	128

parameter space increases the chance of detection of certain types of sinks. Comparing the results of tests #3 and #4 shows that it is a better strategy to increase n_{par} instead of n_{skip}. In both test the same total number of iterations (n_{par} n_{init} n_{skip}) of the Hénon map is computed. However, in the test #4, where n_{par} is larger and n_{skip} is smaller, the number of periodic windows found is larger ($n_{\text{win}}=101$ for the test #4, and $n_{\text{win}}=73$ for the test #3). Similar conclusions can be obtained for other groups of tests.

Now, let us compare the results obtained for different search intervals of the same length. In tests #5, 20, 28, and 30, four different search intervals of length $2 \cdot 10^{-4}$ were considered, and all other parameters of the search procedure are the same. Let us note that the result n_{win} in all cases is in the same range ($n_{\text{win}}=134$, 185, 153, 128). On the other hand, the result n_{sink} changes considerably ($n_{\text{sink}}=8502$, 159835, 548148, and 548148 in tests #5, 20, 28, and 30, respectively). This is related to the existence of wide periodic windows. For example there is a window of width $3.2 \cdot 10^{-9}$ corresponding to period-18 sink in the interval $1.^{4001}_{3999} \times 0.3$. In the interval $1.4 \times 0.^{3001}_{2999}$ there are two windows of width $1.67 \cdot 10^{-7}$ and $3.2 \cdot 10^{-9}$ corresponding to period-19 and period-18 sinks, and in the interval $1.^{4001}_{3999} \times 0.3001$ there are two period-19 windows of widths $1.6 \cdot 10^{-7}$ and $1.7 \cdot 10^{-7}$.

B. Primary and secondary sinks

In order to discuss the structure of sink regions let us define the notions of a primary and secondary sinks. We say that a period-p sink is *secondary* if its region of existence is close and parallel to the region of existence of a sink with period q being a proper divisor of p, and the corresponding stable periodic orbits are close in the state space. We say that a sink is *primary* if it is not secondary. The corresponding regions of existence/periodic windows are also called primary and secondary. Note that if the period of a sink is a prime then the sink is primary. However, the opposite statement is not true. There could be primary sinks with periods being composite numbers. Primary sinks are the core of the structure of sink existence regions. The simplest example of a secondary sink is a period-$2p$ sink born via the period-doubling bifurcation from a period-p sink. In this case, the primary and the secondary sinks have a common border. In theory there could be an infinite sequence of period-doubling bifurcations occurring in a bounded region of the parameter space. In simulations, we usually observe only a few of the shortest sinks with the widest existence regions. In addition to these secondary sinks, we also sometimes observe secondary sinks whose period is a triple (or quintuple, etc.) of the period of the primary sink. Their regions are separated from the regions of existence of period-doubling secondary sinks by regions of chaotic behavior. These secondary sinks also may undergo period-doubling bifurcations leading to more complex secondary sinks.

As an example, in Table II we show the regions of existence of a primary sink and several of its secondary sinks. The primary sink has period 18 (this is the only period-18 sink we found in the region of interest). Secondary sinks have periods 36, 72, 144, 90, 54, 90, 72, 90. The regions of existence have been found non-rigorously using the continuation method. Note that the diameters of the periodic windows change considerably. The first three secondary sinks are generated via the period-doubling bifurcation and have common borders. Others are separated by regions of possibly

TABLE II. Periodic windows for $b=0.3$ close to the period-18 primary sink.

P	a	diam(a)
18	$1.3999769^{131037}_{098966}$	$3.2 \cdot 10^{-9}$
36	$1.399976914^{47073}_{31037}$	$1.6 \cdot 10^{-9}$
72	$1.39997691^{50861}_{46884}$	$4.0 \cdot 10^{-10}$
144	$1.3999769915^{16936}_{07748}$	$9.2 \cdot 10^{-11}$
90	$1.399976915^{2113}_{0818}$	$1.3 \cdot 10^{-11}$
54	$1.399976916^{7044}_{1102}$	$5.9 \cdot 10^{-11}$
90	1.3999769166^{818}_{569}	$2.5 \cdot 10^{-12}$
72	1.3999769169^{530}_{214}	$3.2 \cdot 10^{-12}$
90	1.399976917066^{18}_{00}	$1.9 \cdot 10^{-13}$

chaotic behavior. Similar structures have been observed in other regions of the parameter space (compare Ref. 8).

In order to identify primary periodic windows in the search results we have performed the following computations. As mentioned above, each periodic window with a prime period is primary. When the period is a composite number, we first check whether any sink found previously can be its primary sink. If none of the sinks satisfied the corresponding criteria, we perform a local search for a primary sink in a neighborhood of the current periodic window along the same interval in which the sink was found. When a primary periodic window is detected, it is added to the list. Several new primary sinks have been found in this way. The results are collected in Table III. For each of the four intervals of length $2 \cdot 10^{-4}$ we give the total number of periodic windows and the number of primary periodic windows. Note that the numbers in the second column of the table are larger than the corresponding results in Table I. For example, for the interval $1._{3999}^{4001} \times 0.2999$ eight new primary windows have been found, and the total number of sinks is $136 = 128 + 8$.

The positions at which sinks have been detected are shown in Fig. 2. Points with sinks with periods $p \le 21$ are labelled. Note that more than one point may correspond to a single sink's existence region. For example, there are two points $(a,b) = (1.4,0.299987128)$, $(a,b) = 1.3999769099,0.3)$ at which period-18 sinks were found, but they belong to one region of existence which is a narrow stripe enclosing both points.

C. Continuation method for locating sink existence regions

In order to find regions of existence and identify different regions we have applied the continuation procedure presented in Sec. II C to all 693 primary and secondary sinks found. With a few exceptions, we were able to continue to the border of the rectangle $(a,b) \in [1.3999, 1.4001] \times [0.2999, 0.3001]$. In most cases the existence region was found to be a stripe extending between two edges of the rectangle. There were three exceptions, which will be discussed later. We identified 461 different regions including 210 primary regions. Primary existence regions are shown in Fig. 3. Each region is labelled with the period of the corresponding sink. Observe that the existence regions are narrow stripes and that there are groups of stripes parallel or almost parallel to each other. The groups are plotted using different colors.

Note that there is some ambiguity in the definition of a primary sink, which is related to the fact that the meaning of the word "close" is not precisely defined. We have used the interpretation that if the regions are visually indistinguishable we say they are close. On the other hand there are regions which satisfy other properties of secondary regions but are far from the corresponding primary regions. Examples can be seen in the upper-right corner of Fig. 3, where there exist two regions labelled "38," which are parallel to the period-19 region.

TABLE III. Total number n_{win} of periodic windows and the number n_{pr} of primary periodic windows found in four search intervals.

$a \times b$	n_{win}	n_{pr}
$1._{3999}^{4001} \times 0.3$	173	78
$1.4 \times 0._{2999}^{3001}$	221	106
$1._{3999}^{4001} \times 0.3001$	163	72
$1._{3999}^{4001} \times 0.2999$	136	73
Total	693	329

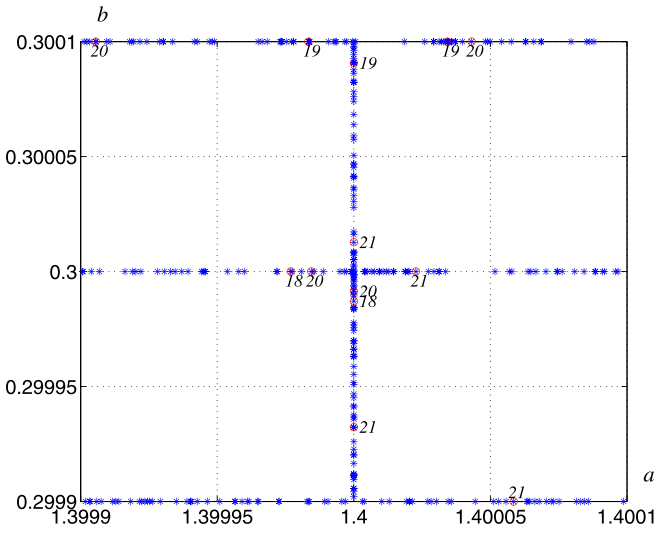

FIG. 2. Points (a,b) at which sinks have been detected along the four lines.

Part of the plot containing the rectangle $(a,b) \in [1.39999, 1.40001] \times [0.29999, 0.30001]$ is shown in Fig. 4. There are 82 regions including 36 primary regions in this rectangle.

D. Properties of sink existence regions

Properties of selected primary regions are given in Table IV. We report results for all regions with period $p \le 21$. For longer periods one region for each period is chosen—we select the region closest to the point (1.4,0.3). We report parameter values (a,b) for which the existence of a

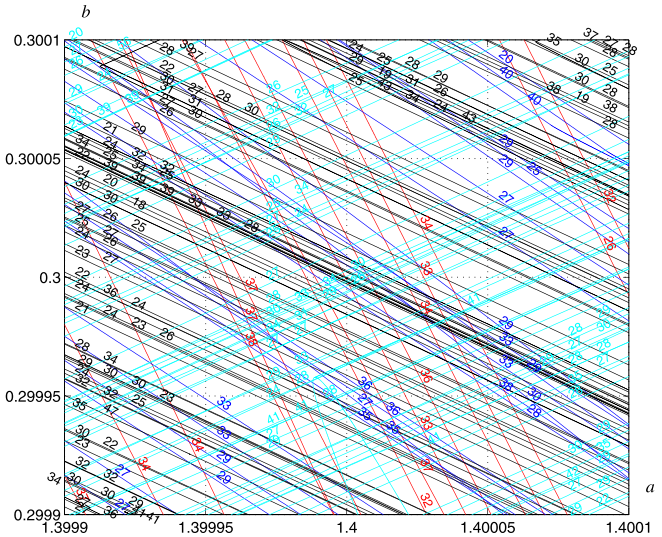

FIG. 3. Regions of existence of primary sinks in the rectangle $(a,b) \in [1.3999, 1.4001] \times [0.2999, 0.3001]$.

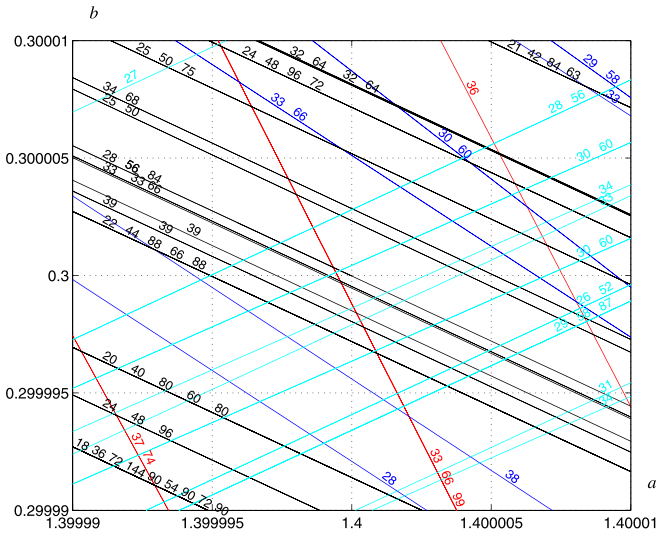

FIG. 4. Regions of existence of primary and secondary sinks in the rectangle $(a,b) \in [1.39999, 1.40001] \times [0.29999, 0.30001]$.

sink was proved, the period p of the sink, the Euclidean distance d between (a,b) and (1.4,0.3), and the width d of the existence region at the point (a,b). The width was found by continuing from the point (a,b) in the directions $(\Delta a, \Delta b) = \pm(\partial\lambda_1/\partial a, \partial\lambda_1/\partial b)$, as described in Sec. II C. Next, we have found in this interval the position of the point where $|\lambda_1|$ achieves the minimum, where λ_1 is the larger (in absolute value) eigenvalue of the Jacobian matrix (4) computed along the orbit. Other results are reported for the point with the minimum value of $|\lambda_1|$. This includes the minimum immediate basin radius r_ε and the immediate basin area s_ε.

Let us now present statistical data based on the 461 sink existence regions found. Fig. 5 shows the number of sinks found for each period. We show the number of primary sinks and the total number of sinks. Note that secondary sinks have periods $p \geq 36$. The shortest orbit found is the period-18 sink. As one can see, the number of sinks found initially increases with the period and for $p > 28$ the number of sinks found starts to decrease. With the hypothesis that sink regions densely fill the parameter space in a neighborhood of the classical parameter values, one can expect that the

TABLE IV. Sink existence regions close to $(a,b) = (1.4,0.3)$, p is the period, w is the width of the existence region, λ_1 is the eigenvalue largest in magnitude, r_ε is the minimum immediate basin radius, s_ε is the immediate basin area, d is the distance from the point (1.4,0.3).

	(a,b)	p	w	λ_1	r_ε	s_ε	d
1	(1.3999769098975,0.3)	18	$1.5616 \cdot 10^{-9}$	$1.9683 \cdot 10^{-5}$	$1.4607 \cdot 10^{-9}$	$7.2750 \cdot 10^{-12}$	$2.3090 \cdot 10^{-5}$
2	(1.4,0.30009066023)	19	$8.1985 \cdot 10^{-8}$	$1.0812 \cdot 10^{-5}$	$8.0639 \cdot 10^{-8}$	$1.8110 \cdot 10^{-9}$	$9.0660 \cdot 10^{-5}$
3	(1.40003418556,0.3001)	19	$7.7075 \cdot 10^{-8}$	$-1.0815 \cdot 10^{-5}$	$6.7199 \cdot 10^{-8}$	$1.7828 \cdot 10^{-9}$	$1.0568 \cdot 10^{-4}$
4	(1.39998447659,0.3)	20	$4.3036 \cdot 10^{-10}$	$5.9049 \cdot 10^{-6}$	$4.0765 \cdot 10^{-10}$	$1.3880 \cdot 10^{-12}$	$1.5523 \cdot 10^{-5}$
5	(1.39990560396,0.3001)	20	$6.7987 \cdot 10^{-10}$	$-5.9246 \cdot 10^{-6}$	$5.8702 \cdot 10^{-10}$	$1.9438 \cdot 10^{-12}$	$1.3752 \cdot 10^{-4}$
6	(1.40004308355,0.3001)	20	$8.1952 \cdot 10^{-10}$	$5.9246 \cdot 10^{-6}$	$5.8702 \cdot 10^{-10}$	$1.1941 \cdot 10^{-12}$	$1.0889 \cdot 10^{-4}$
7	(1.400022743275,0.3)	21	$1.1063 \cdot 10^{-10}$	$-3.2342 \cdot 10^{-6}$	$1.1377 \cdot 10^{-10}$	$1.7185 \cdot 10^{-13}$	$2.2743 \cdot 10^{-5}$
8	(1.4,0.29993238744)	21	$2.1406 \cdot 10^{-10}$	$3.2266 \cdot 10^{-6}$	$1.9659 \cdot 10^{-10}$	$4.3428 \cdot 10^{-13}$	$6.7613 \cdot 10^{-5}$
10	(1.399994921843,0.3)	22	$1.7867 \cdot 10^{-11}$	$1.7715 \cdot 10^{-6}$	$1.8374 \cdot 10^{-11}$	$2.4962 \cdot 10^{-14}$	$5.0782 \cdot 10^{-6}$
11	(1.4,0.29993671494)	23	$1.2578 \cdot 10^{-11}$	$-9.6792 \cdot 10^{-7}$	$1.2760 \cdot 10^{-11}$	$1.0507 \cdot 10^{-14}$	$6.3285 \cdot 10^{-5}$
12	(1.4000128910375,0.3)	24	$6.0601 \cdot 10^{-12}$	$5.3144 \cdot 10^{-7}$	$6.1534 \cdot 10^{-12}$	$3.6143 \cdot 10^{-15}$	$1.2891 \cdot 10^{-5}$
13	(1.400004161333,0.3)	25	$1.3091 \cdot 10^{-12}$	$2.9108 \cdot 10^{-7}$	$1.1926 \cdot 10^{-12}$	$1.1682 \cdot 10^{-15}$	$4.1613 \cdot 10^{-6}$
14	(1.40001070815,0.3)	26	$2.5373 \cdot 10^{-12}$	$-1.5943 \cdot 10^{-7}$	$2.4729 \cdot 10^{-12}$	$1.5282 \cdot 10^{-15}$	$1.0708 \cdot 10^{-5}$
15	(1.399977420742,0.3)	27	$7.6310 \cdot 10^{-13}$	$-8.7325 \cdot 10^{-8}$	$6.9015 \cdot 10^{-13}$	$3.0645 \cdot 10^{-16}$	$2.2579 \cdot 10^{-5}$
16	(1.4,0.2999999774905)	28	$1.2404 \cdot 10^{-13}$	$4.7830 \cdot 10^{-8}$	$1.1146 \cdot 10^{-13}$	$5.0709 \cdot 10^{-17}$	$2.2530 \cdot 10^{-8}$
17	(1.40001197567,0.3)	29	$4.9640 \cdot 10^{-12}$	$-2.6197 \cdot 10^{-8}$	$4.2732 \cdot 10^{-12}$	$3.3836 \cdot 10^{-15}$	$1.1976 \cdot 10^{-5}$
18	(1.399999918279126,0.3)	30	$1.5609 \cdot 10^{-13}$	$1.4349 \cdot 10^{-8}$	$1.3376 \cdot 10^{-13}$	$8.7590 \cdot 10^{-17}$	$8.1721 \cdot 10^{-7}$
19	(1.4,0.299989925114)	31	$4.5675 \cdot 10^{-13}$	$-7.8551 \cdot 10^{-9}$	$3.9939 \cdot 10^{-13}$	$2.3813 \cdot 10^{-16}$	$1.0075 \cdot 10^{-5}$
20	(1.399985536811,0.3)	32	$1.8439 \cdot 10^{-12}$	$4.3047 \cdot 10^{-9}$	$1.1926 \cdot 10^{-12}$	$1.3459 \cdot 10^{-15}$	$1.4463 \cdot 10^{-5}$
21	(1.3999994869436,0.3)	33	$1.0230 \cdot 10^{-12}$	$-2.3578 \cdot 10^{-9}$	$6.9015 \cdot 10^{-13}$	$5.3298 \cdot 10^{-16}$	$5.1306 \cdot 10^{-7}$
22	(1.4,0.2999986087693)	34	$1.4303 \cdot 10^{-13}$	$-1.2913 \cdot 10^{-9}$	$1.3376 \cdot 10^{-13}$	$1.6723 \cdot 10^{-16}$	$1.3912 \cdot 10^{-6}$
23	(1.399930625147 92,0.3)	35	$6.6300 \cdot 10^{-14}$	$7.0733 \cdot 10^{-10}$	$4.4794 \cdot 10^{-14}$	$1.4354 \cdot 10^{-17}$	$6.9375 \cdot 10^{-5}$
24	(1.40000755949567,0.3)	36	$6.5795 \cdot 10^{-13}$	$3.8742 \cdot 10^{-10}$	$4.7927 \cdot 10^{-13}$	$2.8198 \cdot 10^{-16}$	$7.5595 \cdot 10^{-6}$
25	(1.399988818205,0.3)	37	$1.5586 \cdot 10^{-12}$	$2.1220 \cdot 10^{-10}$	$9.9382 \cdot 10^{-13}$	$8.7840 \cdot 10^{-16}$	$1.1182 \cdot 10^{-5}$
26	(1.4,0.2999955934368)	38	$2.9630 \cdot 10^{-14}$	$1.1619 \cdot 10^{-10}$	$2.1602 \cdot 10^{-14}$	$4.8086 \cdot 10^{-18}$	$4.4066 \cdot 10^{-6}$
27	(1.4,0.2999980298226)	39	$1.0967 \cdot 10^{-13}$	$6.3652 \cdot 10^{-11}$	$1.1146 \cdot 10^{-13}$	$6.7942 \cdot 10^{-16}$	$1.9702 \cdot 10^{-6}$
28	(1.40002920074,0.3001)	40	$1.4877 \cdot 10^{-12}$	$3.5101 \cdot 10^{-11}$	$8.2818 \cdot 10^{-13}$	$1.6999 \cdot 10^{-15}$	$1.0418 \cdot 10^{-4}$
29	(1.4,0.29996374713205)	41	$4.6387 \cdot 10^{-13}$	$-1.9051 \cdot 10^{-11}$	$3.9939 \cdot 10^{-13}$	$6.9520 \cdot 10^{-16}$	$3.6253 \cdot 10^{-5}$
30	(1.400053043104,0.2999)	42	$2.5773 \cdot 10^{-13}$	$1.0387 \cdot 10^{-11}$	$2.3113 \cdot 10^{-13}$	$2.9855 \cdot 10^{-16}$	$1.1320 \cdot 10^{-4}$
31	(1.4,0.30008613807)	43	$2.9109 \cdot 10^{-13}$	$-5.7648 \cdot 10^{-12}$	$2.7736 \cdot 10^{-13}$	$1.2033 \cdot 10^{-16}$	$8.6138 \cdot 10^{-5}$
31	(1.399990561167,0.2999)	47	$1.9799 \cdot 10^{-13}$	$-5.1162 \cdot 10^{-13}$	$1.9261 \cdot 10^{-13}$	$3.1945 \cdot 10^{-15}$	$1.0044 \cdot 10^{-4}$
32	(1.399930212636,0.3001)	56	$6.0637 \cdot 10^{-13}$	$2.3091 \cdot 10^{-15}$	$5.7512 \cdot 10^{-13}$	$8.8718 \cdot 10^{-14}$	$1.2194 \cdot 10^{-4}$

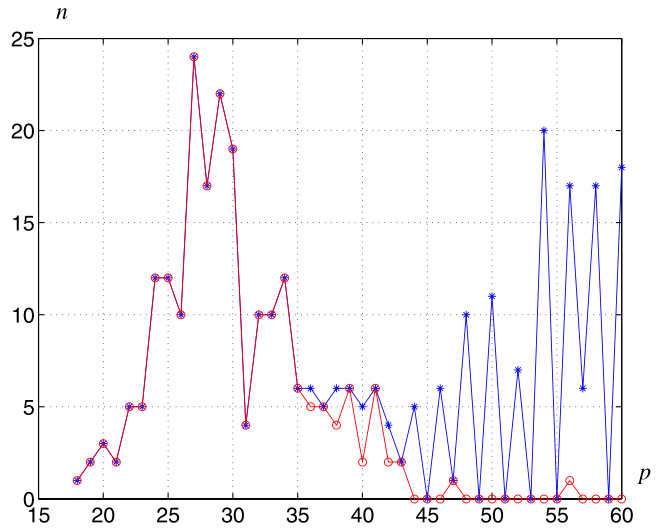

FIG. 5. The number of primary regions (○), and the total number of regions (∗) found for each period p.

number of longer sinks should increase exponentially with the period. This is confirmed, but only for small periods $p \leq 28$, which indicates that perhaps we were not able to find all sinks even for periods close to 30. For periods $p \geq 44$ only two primary sinks were found: one with period 47 and the longest one with period 56 (compare also Table IV). The largest prime period is 47 (for a period-56 sink we cannot be sure that this is indeed a primary sink). Below, we try to explain why in spite of long computations the procedure failed to locate more sinks with longer periods.

Widths of the existence regions versus period are plotted in Fig. 6. The results for primary and secondary regions are shown using the symbols ∗ and ×, respectively. Let us note that widths are in some cases extremely small. In general, for primary sinks the regions for longer orbits are narrower. Regions corresponding to period-19 sinks have largest widths. The smallest width close to $w = 10^{-14}$ is observed for one of the period-39 sinks. This shows that it is necessary to make a very fine sampling of the parameter space to find existence regions corresponding to longer orbits. Observe that

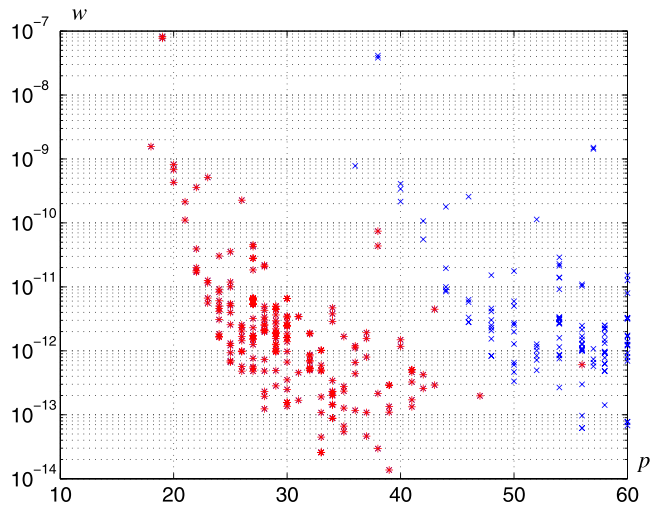

FIG. 6. Widths w of primary (∗) and secondary (×) existence regions versus period p.

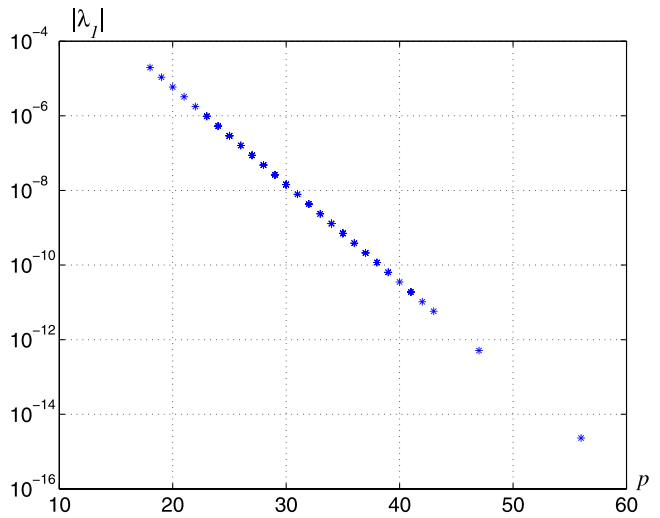

FIG. 7. The absolute value of the larger eigenvalue versus period p.

secondary regions are on average much wider than primary regions with the same period. In a sense, secondary regions inherit the width from their primary regions (widths of secondary regions are only slightly smaller than widths of their primary regions). For example, the period-36 and period-38 secondary sinks have widths a couple of orders of magnitude larger than the primary sinks with the same periods. Two period-38 regions parallel to the period-19 region which as was mentioned earlier are considered as primary regions have widths $(w \in [4 \cdot 10^{-11}, 8 \cdot 10^{-11}])$ in between the period-38 secondary regions $(w \approx 4 \cdot 10^{-7})$ and other period-38 primary regions $(w < 3 \cdot 10^{-13})$.

In Fig. 7, we show the parameter $|\lambda_1|$ characterizing the sink versus the period p. Observe that $\log|\lambda_1|$ decreases linearly with the period. This property can be explained in the following way. Let us recall that $|\lambda_1|$ is calculated at the point of the existence region where $|\lambda_1|$ is minimal. Fig. 8 shows the eigenvalues of the Jacobian matrix when we move across the existence region of one of the period-19 sinks. The values $t = 0$ and $t = 1$ correspond to the borders of the existence region. As one can see $|\lambda_1|$ is minimal at the point where both eigenvalues have the same absolute value. Since

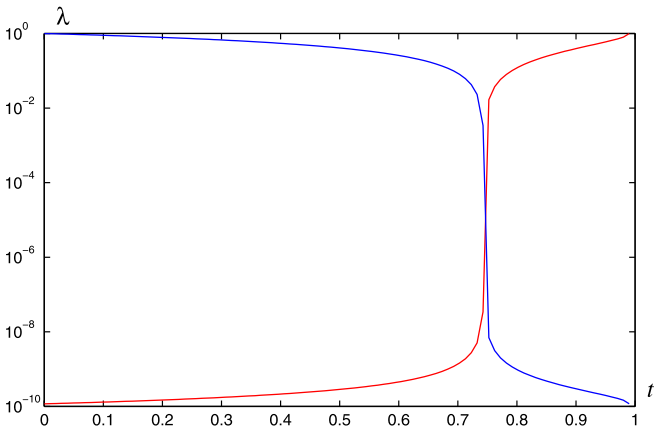

FIG. 8. Eigenvalues of the Jacobian matrix across the existence region of one of the period-19 sinks, $t = 0$ and $t = 1$ correspond to borders of the existence region.

$\lambda_1\lambda_2 = (-b)^p$ it follows that $\log|\lambda_1| = 0.5p\log b$. Since we only consider parameter values close to $b = 0.3$, it follows that the plot should be almost linear in the logarithmic scale.

The minimum immediate basin size and the immediate basin area versus period p are shown in Fig. 9. Note that these two plots are similar, especially for primary sinks. It means that both quantities carry similar information about the immediate basin of attraction. Also note that the first plot for primary sinks is almost identical with the plot of the width of the region of existence. This is a very interesting observation, which means that there is very strong correlation between these two quantities. It follows that the narrower the region of existence is (the lower probability of finding the sink in the parameter space), the smaller immediate basin of attraction of the sink is (the lower probability that after a certain number of iterations a trajectory converges to the sink). Note that for secondary sinks the immediate basin area is larger than for the corresponding primary sinks. This is related to the fact that the number of points belonging to the secondary sink is a multiple of the number of points belonging to the primary sink. In consequence, for fixed parameter values the probability of converging to a secondary sink is higher than the probability of converging to the primary sink. This may be an explanation of the fact that in many cases the search procedure was able to detect a secondary sink and not the corresponding primary sink.

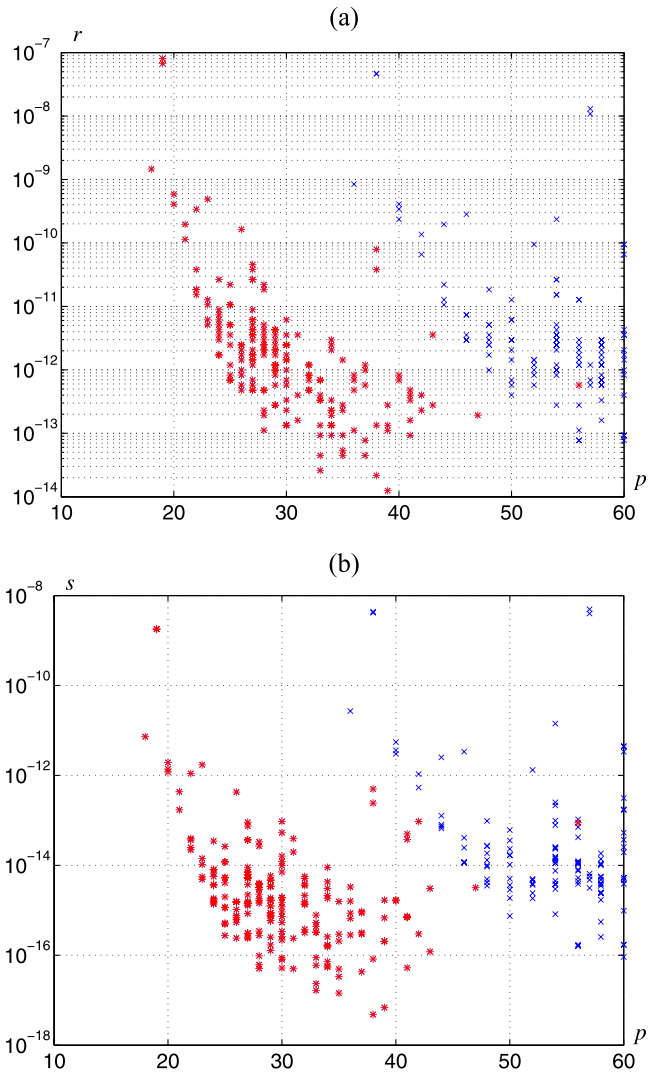

FIG. 9. The minimum immediate basin radius r_ε (a) and lower bound s_ε of the immediate basin area (b) versus period p for primary ($*$) and secondary ($\times$) sinks.

E. Convergence times

Another question of interest is how fast trajectories converge to the found sinks. First, let us consider the point $(a,b) = (1.4,0.2999999774905)$ belonging to the existence region of the period-28 sink passing closest to classical parameter values (see row 16 in Table IV). Its Euclidean distance to (1.4,0.3) is less than $2.3 \cdot 10^{-8}$. Fig. 10 shows two parts of the trajectory of the Hénon map with these parameter values based at the initial condition $(x_0,y_0) = (0,0)$. The first part of the plot is obtained by skipping 10^{10} iterations and plotting the next 10 000 iterations. The plot looks like the classical Hénon attractor observed for $a = 1.4$, $b = 0.3$. In spite of the fact that a huge number of iterations have been skipped the trajectory has not reached the steady state yet. The second part, also composed of 10 000 points is obtained by skipping $1.05 \cdot 10^{10}$ iterations. This second part shows the steady state of the system, which is a period-28 sink. This example shows that it might be necessary to wait very long until the steady state is observed. This long transient is related to the very small minimum immediate basin radius of the sink. A chaotic transient has very low probability of falling into the immediate basin, although in case of a single attractor, eventually it will happen with probability one. It follows that what we observe in many examples reported in the literature, and what is claimed to be a chaotic trajectory, might in fact be a transient to a periodic steady state.

Clearly, the convergence time depends on the initial point. When the initial point belongs to the immediate basin of attraction, the convergence time is 0. To compute the average convergence time we performed the following test. 100 000 random initial conditions were selected, and in each case the convergence time was recorded. The shortest convergence time was 4 723 865 and the longest convergence

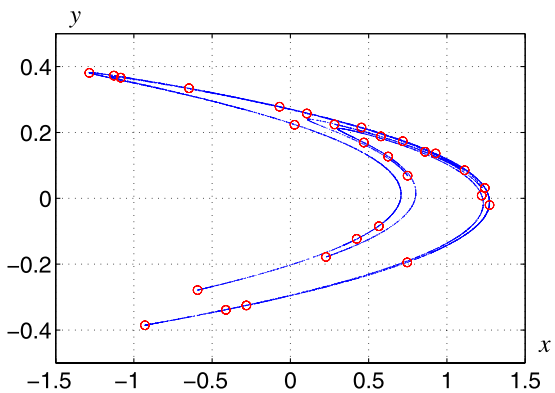

FIG. 10. Trajectory of the Hénon map with $(a,b) = (1.4,0.2999999774905)$ computed in the double-precision arithmetic for the initial condition $(x_0, y_0) = (0,0)$, 10 000 points after skipping 10^{10} iterations are plotted using blue dots, 10 000 points after skipping 1.05×10^{10} iterations are plotted using red circles, chaotic transient is observed for more than 10^{10} iterations; eventually, the trajectory converges to the period-28 sink.

time was above 10^{11}. From this data set one can compute the number of iterations $n_{\text{conv}}(p)$ which are required to converge to the sink with probability p. For example $n_{\text{conv}}(0.5) \approx 1.44 \cdot 10^{10}$, $n_{\text{conv}}(0.9) \approx 4.74 \cdot 10^{10}$.

Similar computations were performed for the point $(a,b) = (1.3999769102,0.3)$, for which a period-18 sink exists and for the point $(a,b) = (1.3999994869436,0.3)$ with a period-33 sink. For the period-18 sink, the shortest and the longest convergence times are 82 and 61392634 iterations, respectively. The convergence probabilities $n_{\text{conv}}(0.5) \approx 3.35 \cdot 10^6$, $n_{\text{conv}}(0.9) \approx 1.11 \cdot 10^7$ are approximately 4000 times smaller than for the period-28 sink. For the period-33 sink the shortest convergence time was 26971 and the convergence probabilities are $n_{\text{conv}}(0.5) \approx 1.66 \cdot 10^9$, $n_{\text{conv}}(0.9) \approx 5.51 \cdot 10^9$. Convergence probabilities are closely related to the minimum immediate basin radius (compare Table IV, rows 1, 16, and 21), which is $r_\varepsilon = 1.4607 \cdot 10^{-9}$, $r_\varepsilon = 6.9015 \cdot 10^{-13}$, and $r_\varepsilon = 1.1146 \cdot 10^{-13}$, for period-18, period-33, and period-28 sinks, respectively.

The number N_k of initial points with the convergence time in the interval $[2^{k-1}, 2^k)$ is shown in Fig. 11. For the period-28 sink, the maximum is for $k = 35$, which means that most trajectories converge after $[2^{34}, 2^{35}) \approx (1.7 \cdot 10^{10}, 3.4 \cdot 10^{10})$ iterations. For other cases, the plots are similar. The difference is that they are shifted towards lower values of k.

F. Structure of the sink existence regions

As one can see in Fig. 3, existence regions in most cases are narrow stripes intersecting with each other. At each intersection, there is a small parallelogram where two sinks coexist. As an example, that this statement is true, we have shown that the point $(a,b) = (1.39999958226963, 0.30000020920279)$ belongs to the intersection of the period-28 and period-30 regions (compare Fig. 4). More precisely, we have proved that there exist period-28 and period-30 sinks for this point in the parameter spaces. The distance from this point to the point (1.4,0.3) is less than $4.68 \cdot 10^{-7}$. In theory, it is also possible that three sinks coexist. This

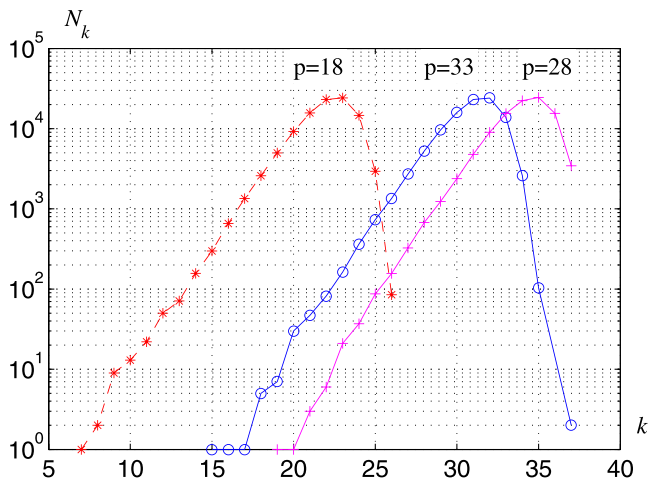

FIG. 11. The number N_k of random initial points with the convergence time in the interval $[2^{k-1}, 2^k)$; $(a,b) = (1.3999769102,0.3)$, period-18 sink (∗); $(a,b) = (1.3999994869436,0.3)$, period-33 sink, (○); $(a,b) = (1.4,0.2999999774905)$ period-28 sink, (+).

phenomenon was confirmed in Ref. 8 for other regions of the parameter space. However, since close to the point (1.4,0.3) the existence regions are extremely thin, a probability of finding a point with 3 coexisting sinks is very low. In fact, we failed to locate such a point. The closest two intersection points were found in a neighborhood of (1.40002701, 0.2999842) at the intersection between the region of existence of a period-29 sink and regions of period-33 and period-34 sinks (see Fig. 3). The distance $2.27 \cdot 10^{-10}$ between the intersection points is quite large when compared to the widths of the corresponding regions, which are close to 10^{-13}.

Looking at Figs. 3 and 4 one can clearly see that existence regions form patterns of parallel lines. One can classify regions by their angles with respect to the axes, and this idea was used to color the figures. Now, we will study the relation between positions of sinks and angles of the corresponding existence regions. First, let us recall that for given parameter values there are many periodic orbits. The number of period-p orbits grows exponentially with the period. This property was confirmed for classical parameter values in Refs. 13 and 17. However, as it is shown in this study, it is very difficult to find a sink. Therefore, one may expect that the most restrictive condition for the existence of a sink is the one involving eigenvalues of the Jacobian matrix (4). Since the Jacobian matrix of the Hénon map depends on x only, it follows that eigenvalues of (4) are functions of values $x_0, x_1, \ldots, x_{p-1}$ and their cyclic order (matrix multiplication is not commutative, but eigenvalues of the Jacobian matrix along the orbit do not depend on the initial point).

Fig. 12(a) shows a period-28 and a period-33 sink existing for $(a,b) = (1.39999995942006,0.3)$ and $(a,b) = (1.3999991587739,0.3)$, respectively. These two points belong to the period-28 and period-33 black parallel regions passing close to the center of Fig. 4. Fig. 12(b) shows a period-26 and a period-29 sink existing for $(a,b) = (1.4,0.2999940739782)$ and $(a,b) = (1.4,0.299993405894)$, belonging to the period-26 and period-39 cyan parallel regions located in the lower half of Fig. 4. The two pairs of regions intersect close to the point $(a,b) = (1.400005, 0.299997)$.

As one can see, the orbits occupy different areas in the state space, which is clearly visible by comparing extreme values of the state variables. Thus, for this example we have confirmed that different angles between the existence regions and the axes are related to the positions of the corresponding sinks. In order to further study this relation let us compare the symbolic representations of the orbits. To represent the orbit $(x_0, x_1, \ldots, x_{p-1})$ we will use the symbol sequence $s = (s_0, s_1, \ldots, s_{p-1})$ defined by $s_k = 0$ for $x_k < 0$ and $s_k = 1$ for $x_k \geq 0$. The symbolic representations of the four sinks shown in Fig. 12 are collected in Table V. The table also presents the symbol sequence of a sink observed in a period-39 region parallel to period-28 and period-33 regions, and the symbol sequence of a sink observed in a period-30 region parallel to period-26 and period-29 regions.

Table VI presents results on the longest common cyclic subsequences for sequences from Table V. One can see that sinks for which existence regions are parallel share longer

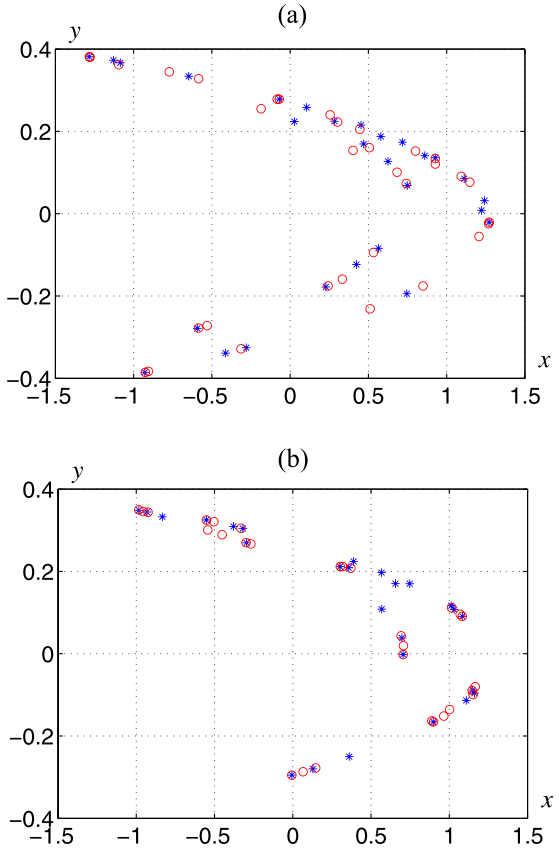

FIG. 12. (a) Period-28 sink for $(a,b) = (1.39999995942006,0.3)$ $(*)$ and period-33 sink $(a,b) = (1.3999991587739,0.3)$ $(\bigcirc)$, (b) period-26 sink for $(a,b) = (1.4,0.2999940739782)$ $(*)$ and period-29 sink $(a,b) = (1.4,0.299993405894)$ $(\bigcirc)$.

common subsequences. In some cases lengths of the longest common subsequences are close to the length of the full sequence. These observations may be helpful in finding sinks with longer periods by limiting the search to periodic orbits with symbolic representations containing specific subsequences only.

Another interesting phenomenon is the existence of close (in some cases visually indistinguishable) parallel primary regions with the same period. Three such examples with periods 32, 33, and 39, respectively, can be seen in Fig. 4 and more are present in Fig. 3. As an example let us consider the two period-32 regions located in the upper-right part of Fig. 4. The intersections of these existence regions with the line $a = 1.4$ are intervals $1.4 \times 0.300008095{95}^{2131}_{1519}$ and $1.4 \times 0.30000815086{1}^{851}_{241}$. The periodic window widths

TABLE V. Symbol sequences of sinks belonging to different groups of parallel regions.

p	s
28	$(1^6010^31^401^30^21^50^2)$
33	$(1^501^20^10^31^40^10^31^401010^2)$
39	$(1^50^10^31^401010^21^40^10^31^401010^2)$
26	$(1^70^10^21^30^1010^1010)$
29	$(1^40^1010^4010101010^21^301010)$
30	$(1^60^1010^10^21^60^21^301010)$

TABLE VI. Lengths of the longest common cyclic subsequence for sequences from Table V.

	28	33	39	26	29	30
28	28	15	16	10	7	10
33	15	33	28	9	10	12
39	16	28	39	9	10	12
26	10	9	9	26	24	15
29	7	10	10	24	29	15
30	10	12	12	15	15	30

are approximately $6 \cdot 10^{-13}$ and the distance between them is slightly less than $5.5 \cdot 10^{-8}$. An interesting question is whether the corresponding sinks are close to each other in the state space.

Fig. 13(a) shows positions of the sinks in the state space. One can see that the sinks are close to each other. The maximum distance between these two orbits achieved at the point $(x,y) = (-0.07524885459802,0.23919215660730)$ is approximately 0.017, but most points along the orbit are visually indistinguishable. Therefore, it is possible that these sinks can be obtained one from another using the continuation method. In an attempt to verify this hypotheses we have continued the sink existing for $(a,b) = (1.4,0.300008095952)$ to $(a,b) = (1.4,0.3000081508615)$ and proved the existence of a

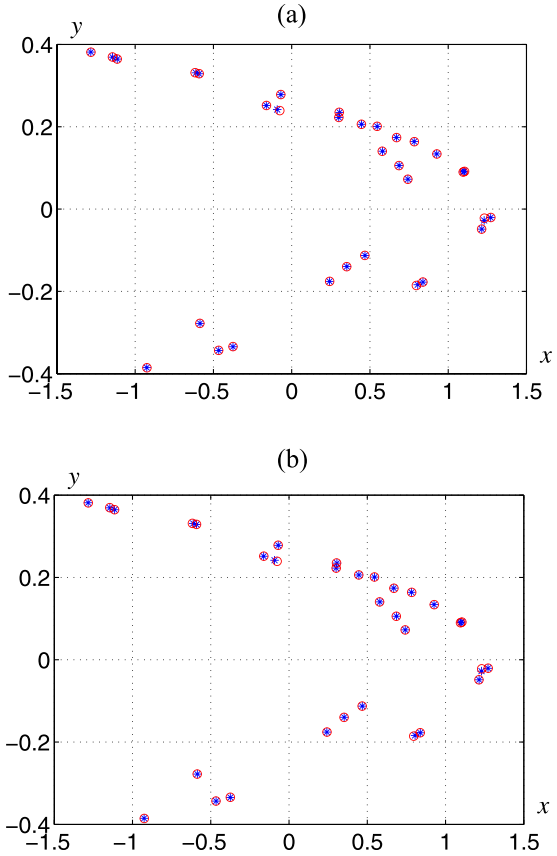

FIG. 13. (a) Period-32 sinks for $(a,b) = (1.4,0.3000081508615)$ $(\bigcirc)$ and $(a,b) = (1.4,0.300008095952)$ $(*)$, (b) stable $(\bigcirc)$ and unstable $(*)$ period-32 orbits for $(a,b) = (1.4,0.3000081508615)$, the unstable sink was obtained using the continuation method from the stable sink for $(a,b) = (1.4,0.300008095952)$.

period-32 orbit at the endpoint of the continuation interval. The orbit is shown in Fig. 13(b) (symbol "$*$"). Its position is very close to the position of the original sink (compare Fig. 13(a)), which is related to very little parameter variation. However, it is different from the sink existing for these parameter values, and hence the hypothesis is false. Moreover, this period-32 orbit is unstable. Note that we have found two period-32 orbits which are very close to each other. They have the same symbolic representation (all pairs of points along the orbits are on the same side of the line $x=0$). The symbol sequence is $s=(1^7 01010^2 1^4 010^3 1^4 01010^2)$. This is another example showing that the symbolic dynamics defined using the sign of x is not unique (compare Ref. 17).

G. Other existence regions

In most cases the existence regions are narrow stripes crossing the region of interest. There are some exceptions, which will be discussed now.

Let us first consider the period-35 regions, which can be seen in the upper-right corner of Fig. 3. At first sight, it looks like two intervals with a common endpoint. A blowup in Fig. 14(a) reveals that in fact the plot contains three branches. This plot was obtained using the continuation method designed for narrow stripes started at two distinct

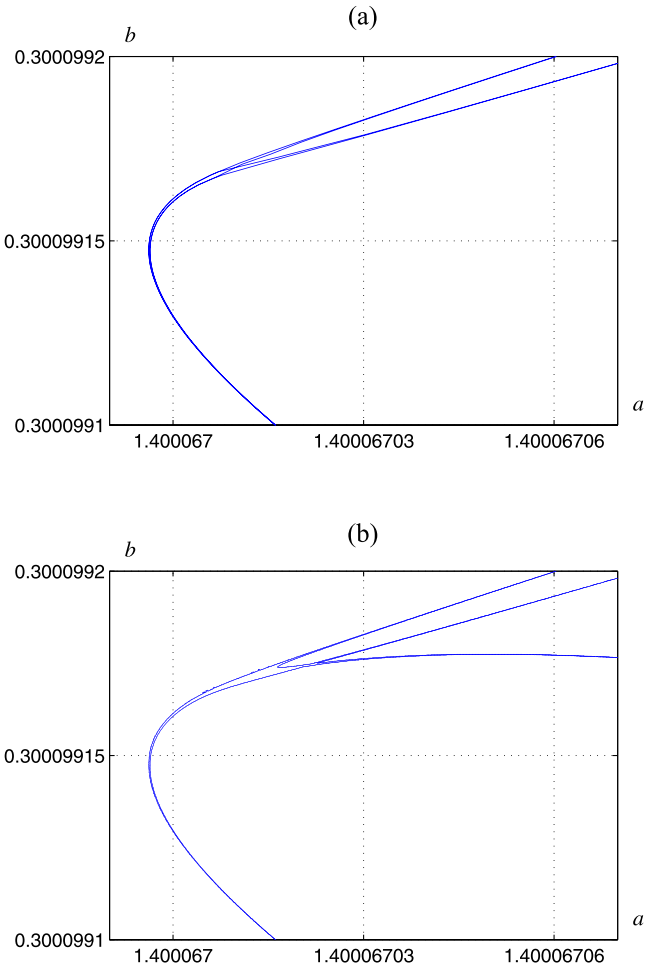

FIG. 14. Border of the period-35 complex existence region found using (a) the continuation method designed for narrow stripes and (b) grid continuation method.

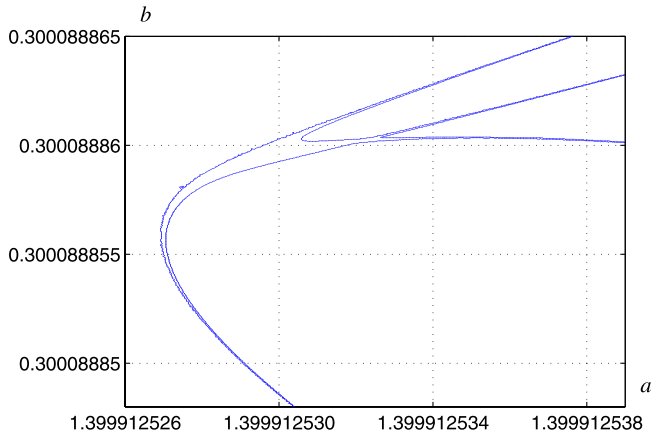

FIG. 15. Border of the period-39 complex existence region.

points (each with a period–35 sink) belonging to the interval $[1.3999, 1.4001] \times \{0.3001\}$. In this plot two upper branches join and form the third branch. This is however not the full picture.

The complete existence region presented in Fig. 14(b) contains four branches forming the swallowtail structure (compare Refs. 8 and 18). It was obtained by a combination of two continuation methods. First, the general method working for regions of arbitrary shape was used to find the existence region in a neighborhood of the point of branch intersection. Then, once points in each branch were identified, the continuation method working for narrow stripes was used to continue into each branch separately. The fact that one of the branches is not present in Fig. 14(a) is due to the way how the method designed for narrow regions works. Continuation along two upper branches ends in both cases in the lower branch, and in consequence the horizontal branch visible in Fig. 14(b) is not found.

Similar computations were carried out for the period-39 region present in the upper-left corner of Fig. 3. The existence region presented in Fig. 15 also has four branches forming a swallowtail structure.

Another complex structure is the period-41 sink existence region. One can see three branches of this region in the lower part of Fig. 3. A blowup shown in Fig. 16 reveals that the region contains four branches. In this case the search

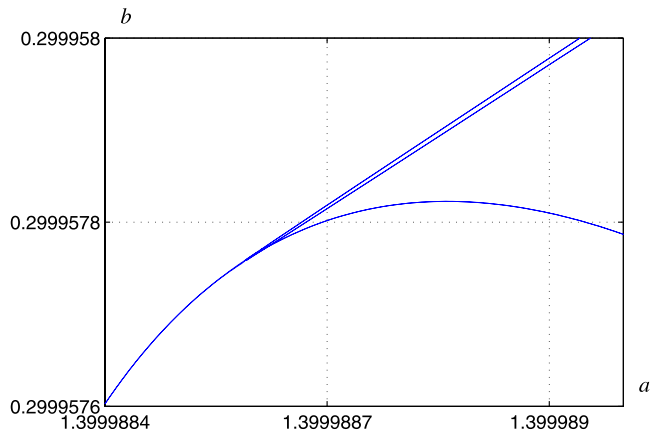

FIG. 16. Period-41 complex existence region.

procedure found all four branches of the (deformed) swallowtail structure, and there is no need to run the general version of the continuation procedure. Note that two of the branches are almost parallel and very close to each other. These two branches are visually indistinguishable in Fig. 3. The distance between the intersections of these two branches with the straight line $a = 1.4001$ is approximately $5.7 \cdot 10^{-8}$. This example shows what can be the origin of very close parallel existence regions corresponding to orbits with the same period.

IV. CONCLUSION

We have located several regions in parameter space for which the Hénon map has a sink. Also, we have demonstrated that there exist low-period sinks extremely close to the classical case; for $(a,b) = (1.4,0.2999999774905)$ there exist a period-28 sink. Thus by varying the parameter b less than $2.3 \cdot 10^{-8}$ from its classical value $\bar{b} = 0.3$, the attractor is a periodic sink. We have also investigated how long transient pieces of trajectories must be computed before the true underlying dynamics is revealed. Based on this, our conclusion is that most numerical studies to this date do not display anything but transient behaviour and are therefore inconclusive as to the true nature of the long-term dynamics of the Hénon map.

The results obtained also indicate that two effects which increase the difficulty to find a sink happen simultaneously. At the same time as the width of the existence region (in parameter space) decreases, the minimum immediate basin size (in phase space) of the corresponding sink becomes smaller. We have illustrated that the minimum immediate basin size decreases exponentially with the period of the sink.

In our future work, we will employ multi-precision computations with the goal of finding additional sinks for parameters significantly closer to the classical parameter values. Ultimately, we aim to establish the stated conjecture.

ACKNOWLEDGMENTS

This work was supported in part by the AGH University of Science and Technology (Grant No. 11.11.120.343) and the Swedish Research Council (Grant No. 2005-3152). Part of the computations reported in this work were performed at ACK CYFRONET AGH, computational Grant No. MNiSW/Zeus_GPGPU/AGH/058/2011.

[1]M. Hénon, Commun. Math. Phys. **50**, 69 (1976).
[2]M. Jakobson, Commun. Math. Phys. **81**, 39 (1981).
[3]J. Graczyk and G. Swiatek, Ann. Math. Second Ser. **146**, 1 (1997).
[4]M. Lyubich, Ann. Math. Second Ser. **156**, 1 (2002).
[5]M. Benedicks and L. Carleson, Ann. Math. **133**, 73 (1991).
[6]S. Newhouse, Publ. Math. Inst. Hautes Etudes Sei. **50**, 101 (1979).
[7]C. Robinson, Commun. Math. Phys. **90**, 433 (1983).
[8]Z. Galias and W. Tucker, Int. J. Bifurcation Chaos **23**, 1330025 (2013).
[9]Z. Galias and W. Tucker, in *Proceedings of IEEE International Symposium on Circuits and System, ISCAS'13* (Beijing, 2013), pp. 2571–2574.
[10]R. Moore, *Interval Analysis* (Prentice Hall, Englewood Cliffs, NJ, 1966).
[11]A. Neumaier, *Interval Methods for Systems of Equations* (Cambridge University Press, 1990).
[12]Z. Galias, Int. J. Bifurcation Chaos **16**, 2873 (2006).
[13]Z. Galias, Int. J. Bifurcation Chaos **11**, 2427 (2001).
[14]Z. Galias, IEEE Circuits Syst. Mag. **13**, 35 (2013).
[15]E. Allgower and K. Georg, SIAM Rev. **22**, 28 (1980).
[16]E. Barreto, B. Hunt, C. Grebogi, and J. Yorke, Phys. Rev. Lett. **78**, 4561 (1997).
[17]O. Biham and W. Wenzel, Phys. Rev. Lett. **63**, 819 (1989).
[18]K. Hansen and P. Cvitanović, Nonlinearity **11**, 1233 (1998).